CHAPTER 4

DIELECTRIC RELAXATION PHENOMENA OF SOME APROTIC POLAR LIQUIDS UNDER GIGA HERTZ ELECTRIC FIELD

4. DIELECTRIC RELAXATION PHENOMENA OF SOME APROTIC POLAR LIQUIDS UNDER GIGA HERTZ ELECTRIC FIELD

4.1. INTRODUCTION

The relaxation behaviour of polar-nonpolar liquid mixtures under high frequency (hf) electric field is of much importance to study the molecular shapes, sizes as well as associational behaviours [1-3] in them. Workers in this field usually analyse the experimental data obtained through relaxation mechanisms involved on the basis of various models [4-6] applicable to polar liquids. Dhull et al [7] and Sharma & Sharma [8] had, however, measured the real ε'_{ijk}, ε'_{ij} or ε'_{ik} and imaginary ε''_{ijk}, ε''_{ij} or ε''_{ik} parts of relative complex permittivities ε_{ijk}^*, ε_{ij}^* or ε_{ik}^* of some interesting binary or single polar liquids (jk, j or k) in a nonpolar solvent under X-band electric field at different or fixed temperatures. The purpose of the work was to detect monomer (solute–solvent) or dimer (solute–solute) molecular associations and molecular dynamics of the systems in terms of estimated relaxation time τ_j and dipole moment μ_j.

The measured [9] values of the relative permittivities ε_{ij}'s of some aprotic polar liquids like N,N-dimethylsulphoxide (DMSO); N,N–dimethylformamide (DMF); N,N–dimethyl acetamide (DMA) and N,N–diethylformamide (DEF) in benzene under the most effective dispersive region of nearly 10 GHz electric field at 25, 30, 35 and 40°C for DMSO; 25°C for DMA and DMF and 30°C for DEF respectively. DMSO is a aprotic dipolar liquid of high penetrating power and wide application in medicine and industry. It acts as good constituent of binary mixtures because of its associative [10] nature. Amides, on the other hand, are the building blocks of proteins and enzymes and have wide biological applications. The liquids usually show two relaxation times τ_2 and τ_1 for the rotation of the whole molecules and the flexible parts attached to the parent molecules from the single frequency measurement technique. [11-12]

All these facts inspired us to study τ_2 and τ_1 and dipole moments μ_2 and μ_1 of these liquids in terms of real χ'_{ij} $(=\varepsilon'_{ij}-\varepsilon_{\infty ij})$ and imaginary χ''_{ij} $(=\varepsilon''_{ij})$ parts of complex orientational susceptibility χ_{ij}^* $(=\varepsilon_{ij}^*-\varepsilon_{\infty ij})$ in benzene at different temperatures. The low frequency susceptibility χ_{0ij} $(=\varepsilon_{0ij}-\varepsilon_{\infty ij})$ is however real. χ'_{ij} can be obtained by subtracting either 1 or $\varepsilon_{\infty ij}$ from the measured ε_{ij}'s. If 1 is subtracted from the relative permittivity ε'_{ij} and ε_{0ij} one

gets χ'_{ij} and χ_{oij} containing all types of polarisation processes including fast polarization. When high frequency relative permittivity or the optical permittivity $\varepsilon_{\infty ij}$ be subtracted from ε_{ij}' and ε_{oij} of the solution at a certain weight fraction w_j's of the solute the susceptibility χ'_{ij}, χ''_{ij} and χ_{oij} result due to orientational polarisation only. Our earlier study [9] was to calculate τ's and μ's in terms of either relative permittivities ε_{ij}'s or hf conductivities σ_{ij}'s. ε_{ij}'s are involved with all types of polarisations while σ_{ij}'s are related only to bound molecular charges of polar liquids. Nowadays relaxation mechanisms are studied in terms of χ_{ij}'s [13] because measurements of μ's in terms of ε_{ij}'s or σ_{ij}'s include contributions due to all types of polarisations and bound molecular charges respectively. Moreover, relaxation processes are highly thermally activated to yield τ within the framework of Debye–Smith model of polar–nonpolar liquid mixture.

The purpose of the present work is to assess the contribution of fast polarisation and bound molecular charges in the measurement of μ's when compared with μ's from χ_{ij} and σ_{ij} measurements. The variation of μ's with temperature provides knowledge of the state of the system through the measured energy parameters.

The detailed experimental technique involved in the measurement of dielectric relaxation parameters of solution has been described elsewhere [14]. A Hewlett Packard Impedance Analyser (HP–4192A) measured the capacitance and conductance of the cell containing polar–nonpolar liquid mixtures at different frequencies and temperatures for a fixed w_j of solute. The real and imaginary parts of relative permittivities ε_{ij}^* or susceptibility χ_{ij}^* are obtained from complex impedances of the cell measured within the range of frequencies from 5 Hz to 13 MHz. The measured ε_{ij}'s are then plotted in a Cole–Cole semicircular arc to get the values of ε'_{ij}, ε''_{ij}, ε_{oij} and $\varepsilon_{\infty ij}$ at nearly 10 GHz electric field (Table.4.1). Again ε_{oij} is measured at 1 KHz whereas high frequency permittivity $\varepsilon_{\infty ij}$ (= n^2_{Dij}) is measured by Abbe's Refractometer to compare the values obtained from Cole–Cole plot. The cell containing experimental liquid mixture is then kept in Mettler Hot Stage FP–52 chamber to regulate temperature. Multiply distilled C_6H_6 is used as a solvent in measurement after several times fractional distillation to get the purest quality of sample. The measured data ε'_{ij} or χ'_{ij} 's are accurate within $\pm$ 5%.

Bergmann et al [15], however, proposed a graphical technique to get τ_1, τ_2 and c_1, c_2 for a pure polar liquid at different frequencies of the microwave electric field. In order to

avoid clumsiness of algebra and fast polarisation processes, the molecular orientational polarisations in terms of established symbols of χ_{ij}'s can be written as [5]

$$\frac{\chi'_{ij}}{\chi_{oij}} = \frac{c_1}{1+\omega^2\tau_1^{\,2}} + \frac{c_2}{1+\omega^2\tau_2^{\,2}} \tag{4.1}$$

$$\frac{\chi''_{ij}}{\chi_{oij}} = c_1\frac{\omega\tau_1}{1+\omega^2\tau_1^{\,2}} + c_2\frac{\omega\tau_2}{1+\omega^2\tau_2^{\,2}} \tag{4.2}$$

assuming two separate broad Debye type dispersions of which $c_1 + c_2 = 1$.

Saha et al [11] and Sit et al [12] put forward an analytical technique to measure τ_1, τ_2 and c_1, c_2 of a polar–nonpolar liquid mixture in terms of measured χ'_{ij}, χ''_{ij}, χ_{oij} at different w_j's of solute under a single frequency electric field and temperature. eqs (4.1) and (4.2) are solved to get

$$\frac{\chi_{oij}-\chi'_{ij}}{\chi'_{ij}} = \omega(\tau_1+\tau_2)\frac{\chi''_{ij}}{\chi'_{ij}} - \omega^2\tau_1\tau_2 \tag{4.3}$$

The eq. (4.3) gives a straight line when $(\chi_{oij}-\chi'_{ij})/\chi'_{ij}$ is plotted against χ''_{ij}/χ'_{ij} for different w_j's of solute for a given angular frequency ω (= $2\pi f$), f being the frequency of the applied electric field. The slope $\omega(\tau_1+\tau_2)$ and intercept $-\omega^2\tau_1\tau_2$ of straight line of eq. (4.3) are obtained through linear regression analysis as shown in Fig. 4.1. Relaxation times τ_2 and τ_1 are calculated from the slopes and intercepts of eq. (4.3) of Fig. 4.1 in terms of measured data of Table 4.1. They are then compared with measured τ_j's from the linear slope of the χ''_{ij} against χ'_{ij} curve of Fig. 4.2 at different w_j's of the form:

$$\frac{d\chi''_{ij}}{d\chi'_{ij}} = \omega\tau \tag{4.4}$$

Both χ''_{ij} and $\chi'_{ij}$are functions of w_j's of solute. It is better to use the individual slopes χ''_{ij}– w_j and χ'_{ij}– w_j curves in Figs. 4.3 and 4.4 at $w_j \to 0$ to measure τ using the following equation:

$$\frac{\left(d\chi''_{ij}/dw_j\right)_{wj\to 0}}{\left(d\chi'_{ij}/dw_j\right)_{wj\to 0}} = \omega\tau \tag{4.5}$$

τ's from both the methods along with τ's from conductivity measurement technique using eqs. (4.25) and (4.26) [see later] are placed in Table 4.2 in order to compare with τ measured by Gopala Krishna's method [16].

eqs. (4.1) and (4.2) are solved for c_1 and c_2 to get:

$$c_1 = \frac{(\chi'_{ij}\alpha_2 - \chi''_{ij})(1+\alpha_1^{\,2})}{\chi_{oij}(\alpha_2 - \alpha_1)} \tag{4.6}$$

$$c_2 = \frac{(\chi''_{ij} - \chi'_{ij}\alpha_1)(1+\alpha_2^{\,2})}{\chi_{oij}(\alpha_2 - \alpha_1)} \tag{4.7}$$

where $\alpha_1=\omega\,\tau_1$ and $\alpha_2=\omega\,\tau_2$, such that $\alpha_2 > \alpha_1$. The values of χ'_{ij}/χ_{oij} and χ''_{ij}/χ_{oij} are also obtained from following Fröhlich's equations. [17]:

$$\frac{\chi'_{ij}}{\chi_{oij}} = 1 - \frac{1}{2A}\ln\left(\frac{1+\omega^2\tau_2^{\,2}}{1+\omega^2\tau_1^{\,2}}\right) \tag{4.8}$$

$$\frac{\chi''_{ij}}{\chi_{oij}} = \frac{1}{A}\left[\tan^{-1}(\omega\tau_2) - \tan^{-1}(\omega\tau_1)\right] \tag{4.9}$$

where A = Fröhlich parameter = $\ln(\tau_2/\tau_1)$. The theoretical values of relative contributions c_1 and c_2 towards dielectric relaxation processes for τ_1 and τ_2 are computed from eqs.(4.8) and (4.9). They are presented in Table 4.3. The graphical plots of χ'_{ij}/χ_{oij} and χ''_{ij}/χ_{oij} curves as a function of w_j are shown in Figs 4.5 and 4.6 respectively. The experimental values of c_1 and c_2 are also estimated from eqs(4.1) and (4.2) with the measured values of $(\chi'_{ij}/\chi_{oij})\ w_j \to 0$ and $(\chi''_{ij}/\chi_{oij})\ w_j \to 0$ of Figs 4.5 and 4.6. These c_1 and c_2 are finally compared with theoretical ones in Table 4.3.

The symmetric and asymmetric distribution parameters γ and δ of the molecules under study are calculated and placed in the last columns of the Table 4.3 along with all the c_1 and c_2's in order to see that the relaxation mechanism for such liquids are symmetric.

The dipole moments μ_2 and μ_1 due to rotation of the whole molecule as well as the flexible parts of the molecules are determined from the slope β_1 of χ'_{ij}–w_j curve of Fig. 4.4 at $w_j \to 0$ in terms of estimated τ_j of eq. (4.3) as placed in Table 4.4. μ_j's are again calculated from the τ's of eqs. (4.4) and (4.25) of Murthy etal [18] and the ratio of the individual slopes of eqs. (4.5) and (4.26) from susceptibility and conductivity measurements using slope β_1 of χ'_{ij}– w_j of Fig 4.4 and β_2 of σ_{ij}– w_j curve of Fig. 4.7. μ's from both the measurements are entered in Table 4.4 along with estimated μ's from Gopala Krishna's method [16] quoted as reported ones in the Table 4.4.

The variations of measured μ_2 and μ_1 for DMSO in benzene with temperature in ^0C are given by the equations:

$$\mu_2 = -231.61 + 15.597\ t - 0.2272\ t^2$$
$$\mu_1 = 19.825 - 0.626\ t + 0.0108\ t^2 \qquad (4.10)$$

μ_2 of the parent molecule attains a maximum value of 36 C.m at 34.32^0C with zero dipole moments at 21.72 ^0C and 46.92 ^0C respectively due to monomer formation with C_6H_6 ring.

The theoretical dipole moment μ_{theo}'s of the molecules are calculated from the available infrared spectroscopic data of bond moments assuming the molecules are planar as sketched in Fig 4.8. They are found to vary with the measured μ_j's. The difference, however, indicates that the effect of inductive, mesomeric and electromeric moments of the substituent polar groups within the molecules along with temperature in the hf electric field is to be considered to have the conformation of the molecules under interest.

The thermodynamic energy parameters like enthalpy of activation ΔH_τ free energy of activation ΔF_τ and entropy of activation ΔS_τ were obtained from the slope and intercept of linear equation of $\ln(\tau_1 T)$ against 1/T for DMSO as given by the equation.

$$\ln(\tau_2 T) = -4.8353 - 4.088\times10^3(1/T)$$
$$\ln(\tau_1 T) = -30.568 + 3.216\times10^3(1/T) \qquad (4.11)$$

The variation of $\ln(\tau_1 T)$ or $\ln(\tau_2 T)$ against 1/T indicate that τ_1 obeys the Eyring rate process whereas τ_2 does not.

4.2 SYMMETRIC AND ASYMMETRIC DISTRIBUTION PARAMETER γ AND δ

The polar–nonpolar liquid mixtures under study are nonrigid in nature exhibiting two relaxation times τ_2 and τ_1 at a single frequency electric field. [19] The measured values of χ''_{ij}/χ_{oij} when plotted against χ'_{ij}/χ_{oij} at $\omega_j \rightarrow 0$ for different frequency ω at a fixed experimental temperature for DMSO may either show Cole–Cole semicircular arc or Cole–Davidson skewed arc having symmetric and asymmetric distribution of relaxation behaviour according to following equations:

$$\frac{\chi_{ij}^{*}}{\chi_{oij}} = \frac{1}{1+(j\omega\tau_s)^{1-\gamma}} \qquad (4.12)$$

$$\frac{\chi_{ij}^{*}}{\chi_{oij}} = \frac{1}{(1+j\omega\tau_{cs})^{\delta}} \tag{4.13}$$

where τ_s and τ_{cs} are symmetric and characteristics relaxation times related to symmetric and asymmetric distribution parameters γ and δ respectively. On separation the real and imaginary parts of eq. (4.12) one gets:

$$\gamma = \frac{2}{\pi}\tan^{-1}\left[\left(1-\frac{\chi'_{ij}}{\chi_{oij}}\right)\frac{\chi'_{ij}/\chi_{oij}}{\chi''_{ij}/\chi_{oij}} - \frac{\chi''_{ij}}{\chi_{oij}}\right] \tag{4.14}$$

$$\tau_s = \frac{1}{\omega}\left[1\Big/\left(\frac{\chi'_{ij}/\chi_{oij}}{\chi''_{ij}/\chi_{oij}}\cos\frac{\gamma\pi}{2} - \sin\frac{\gamma\pi}{2}\right)\right]^{\frac{1}{1-\gamma}} \tag{4.15}$$

On simplification of eq. (4.13) further one gets :

$$\frac{1}{\phi}\log(\cos\phi) = \frac{\log\left[\left(\chi'_{ij}/\chi_{oij}\right)/\cos(\phi\delta)\right]}{\phi\delta} \tag{4.16}$$

$$\tan(\phi\delta) = \frac{\left(\chi''_{ij}/\chi_{oij}\right)_{wj\to 0}}{\left(\chi'_{ij}/\chi_{oij}\right)_{wj\to 0}} \tag{4.17}$$

where $\tan\varphi = \omega\tau_{cs}$

A theoretical curve of $(1/\phi)\log(\cos\varphi)$ with ϕ in degrees was drawn [5] to get the known values of ϕ and δ in terms of measured parameter of $[\log\{(\chi'_{ij}/\chi_{oij})/\cos(\phi\delta)\}] / (\phi\delta)$ of eqs. (4.16) and (17). All the τ_s, τ_{cs} and δ ϕ are given in Tables 4.2 and 4.3 respectively.

4.3 DIPOLE MOMENT μ_j FROM SUSCEPTIBILITY MEASUREMENT

Debye equation [20] of relative permittivities of a polar solute (j) dissolved in a nonpolar solvent (i) in terms of complex dielectric orientational susceptibility χ^{*}_{ij} of solution can be written as:

$$\frac{\chi_{ij}^{*}}{\chi_{oij}} = \frac{1}{1+j\omega\tau} \tag{4.18}$$

where χ'_{ij} (=$\varepsilon'_{ij}-\varepsilon_{\infty ij}$) and χ''_{ij} (=ε''_{ij}) are the real and imaginary parts of $\chi^*_{ij} = \chi'_{ij}-j\chi''_{ij}$, $j = \sqrt{-1}$ is a complex number χ_{oij} (=$\varepsilon_{oij}-\varepsilon_{\infty ij}$) is the low frequency susceptibility which is real.

Again, the imaginary part of dielectric orientational susceptibility χ''_{ij} as a function of w_j can be written according to Smith [21] as:

$$\chi''_{ij} = \frac{N\rho_{ij}\mu_j^2}{27\varepsilon_o k_B T M_j} \frac{\omega\tau}{1+\omega^2\tau^2} (\varepsilon_{ij}+2)^2 w_j \qquad (4.19)$$

On differentiation of eq. (4.19) w.r. t w_j at $w_j \to 0$ one gets:

$$\left(\frac{d\chi''_{ij}}{dw_j}\right)_{w_j \to 0} = \frac{N\rho_{ij}\mu_j^2}{27\varepsilon_o k_B T M_j} \frac{\omega\tau}{1+\omega^2\tau^2} (\varepsilon_i+2)^2 \qquad (4.20)$$

where k_B = Boltzmann constant, N = Avogadro's Number ε_i = relative permittivity of the solute and ε_o = Absolute permittivitiy of free space = 8.854 X 10^{-12} $F.m^{-1}$, all expressed in S.I. units. Comparing eqs.(4.4) and (4.20) one gets :

$$\left(\frac{d\chi'_{ij}}{dw_j}\right)_{w_j \to 0} = \frac{N\rho_i\mu_j^2}{27\varepsilon_o k_B T M_j} \frac{1}{1+\omega^2\tau^2} (\varepsilon_i+2)^2 = \beta_1 \qquad (4.21)$$

where β_1 is the slope of χ'_{ij}–w_j curves at $w_j \to 0$.

From eq. (4.21) one gets the dipole moment μ_j as:

$$\mu_j = \left(\frac{27\varepsilon_o k_B T M_j \beta_1}{N\rho_i (\varepsilon_i+2)^2 b}\right)^{\frac{1}{2}} \qquad (4.22)$$

where b = $1/(1+\omega^2\tau^2)$ is the dimensionless parameter involved with measured τ_j of Table 4.2. All the μ_j's are placed in Table 4.4.

4.4 DIPOLE MOMENT μ_j FROM hf CONDUCTIVITY MEASUREMENT

The hf complex conductivity σ^*_{ij} of a polar–nonpolar liquid mixture is given by:

$\sigma^*_{ij} = \sigma'_{ij} + j\sigma''_{ij} = \omega\varepsilon_o (\varepsilon''_{ij} + j\varepsilon'_{ij})$ (4.23)

the real σ'_{ij} and imaginary σ''_{ij} parts of σ^*_{ij} are related by

$$\sigma''_{ij} = \sigma_{\infty ij} + \frac{1}{\omega\tau_j}\sigma'_{ij} \tag{4.24}$$

where $\sigma_{\infty ij}$ is the constant conductivity at infinite dilution i.e. at $w_j \to 0$. The eq. (4.24) on differentiation w.r.t. σ'_{ij} yields:

$$\frac{d\sigma''_{ij}}{d\sigma'_{ij}} = \frac{1}{\omega\tau_j} \tag{4.25}$$

which provides a convenient method to obtain τ_j of a polar molecule. It is, however, better to use the ratio of the slopes of variation of σ''_{ij} and σ'_{ij} with w_j in order to avoid polar–polar interactions at $w_j \to 0$ in a given solvent to get τ_j from:

$$\frac{\left(d\sigma''_{ij}/dw_j\right)_{w_j\to 0}}{\left(d\sigma'_{ij}/dw_j\right)_{w_j\to 0}} = \frac{1}{\omega\tau_j} \tag{4.26}$$

In hf region of GHz range, it is generally observed that $\sigma''_{ij} \cong \sigma_{ij}$ the total hf conductivity [22] of the solution. Therefore, the eq. (4.24) can be written as:

$$\sigma_{ij} = \sigma_{\infty ij} + \frac{1}{\omega\tau_j}\sigma'_{ij} \tag{4.27}$$

$$\beta_2 = \frac{1}{\omega\tau_j}\left(\frac{d\sigma'_{ij}}{dw_j}\right)_{wj\to 0}$$

where β_2 is the slope of ($d\sigma_{ij}/d\, w_j$) $_{w_j \to 0}$. The real part σ'_{ij} of a polar–nonpolar liquid mixture is given by [5]

$$\sigma'_{ij} = \frac{N\rho_{ij}\mu_j^{\,2}}{27k_B TM_j}\frac{\omega^2\tau_j}{1+\omega^2\tau_j^2}\left(\varepsilon_{ij}+2\right)^2 w_j$$

$$\left(\frac{d\sigma'_{ij}}{dw_j}\right)_{w_j\to 0} = \frac{N\rho_i\mu_j^{\,2}}{27k_B TM_j}\frac{\omega^2\tau_j}{1+\omega^2\tau_j^2}\left(\varepsilon_i+2\right)^2 \tag{4.28}$$

Now comparing eqs. (4.27) and (4.28) one gets hf μ_j from

$$\mu_j = \left(\frac{27k_B TM_j\beta_2}{N\rho_i\left(\varepsilon_i+2\right)^2\omega b}\right)^{\frac{1}{2}} \tag{4.29}$$

where b=1 / (1+$\omega^2\tau^2$) is involved with τ_j's from eqs. (4.25) and (4.26). μ_j's thus obtained from eq. (4.29) are placed in Table 4.4 along with Gopala Krishna's μ_j and μ_{theo}'s.

4.5 RESULT AND DISCUSSION

The relaxation parameters in terms of real χ'_{ij} (=ε'_{ij}–$\varepsilon_{\infty ij}$), imaginary χ''_{ij} (=ε''_{ij}) and low frequency susceptibility χ_{oij} (=ε_{oij}–$\varepsilon_{\infty ij}$), which is real are extracted from the measured relative permittivities ε_{ij}'s for different w_j's of solute at 25, 30, 35 and 40^{o}C for DMSO, 25^{o}C for DMA and DMF and 30^{o}C for DEF under nearly 10 GHz electric field as shown in Table 4.1. The curves of (χ_{oij}–χ'_{ij})/χ_{ij}' against χ''_{ij}/χ'_{ij} at different w_j's of solute are plotted from the measured data in Fig 4.1. All the curves show two relaxation times τ_2 and τ_1 due to rotation of the whole molecule and the flexible part attached to the parent ones as evident from Table 4.2. It indicates that the molecules are of non-rigid nature. Unlike τ_2's, τ_1's of DMSO at 25, 30, 35 and 40^{o}C decrease gradually (Table 4.2). This indicates that τ_1's obey the Debye relaxation mechanism. It is also evident from Table 4.2 and Fig. 4.1 that the graphs of (χ_{oij}–χ'_{ij})/χ '$_{ij}$ against χ''_{ij}/χ'_{ij} for different w_j's of DMSO shift towards the origin with the increase of temperature. τ_2 's of all the liquids are much larger in magnitude than τ_1. The parent molecule takes larger time to lag with the electric field frequency for its inertia in comparison to its flexible parts which are supported by the two relaxation model of polar unit under nearly 10 GHz electric field [23]. τ_j's are estimated and placed in Table 4.2 from eqs. (4.4) and (4.5) using linear slope of χ''_{ij} against χ'_{ij} at different w_j's and the ratio of individual slopes of χ''_{ij}– w_j and χ'_{ij}– w_j curves at $w_j \rightarrow 0$ of Figs. 4.3 and 4.4 respectively. The values of τ_j from eq. (4.4) are larger than from eq. (4.5). Reported τ's and τ_j's calculated from both the Gopala Krishna's method [16] as well as conductivity measurement technique using eqs. (4.25) and (4.26) respectively. The agreement is better from the τ_j's due to ratio of the individual slopes of χ''_{ij}– w_j and χ'_{ij}– w_j curves at $w_j \rightarrow 0$ of Figs. 4.3 and 4.4 because the polar–polar interactions are almost avoided. They are then compared with the reported τ_s and τ_{cs} of the molecules assuming symmetric and asymmetric distribution of relaxation processes only to show that the molecules obey symmetric distribution. The curves χ''_{ij} against χ'_{ij} of Fig. 4.2 of the molecules are found to meet at a point in the region of $0 < w_j < 0.02$ except DEF the data was measured at 30 ^{0}C. The experimental curves of χ''_{ij}– w_j and χ'_{ij}– w_j are not linear as

shown in Figs. 4.3 and 4.4 respectively. Like χ'_{ij}– w_j curves all the curves of χ''_{ij}– w_j of Fig. 4. 3 are parabolic in nature and increase with the w_j's of solute. The magnitude of χ''_{ij} is, however, maximum in lower temperature region and decrease with the rise of temperature. This indicates the absorption of electric energy in the polar–nonpolar mixture in the lower temperature region.

The relative contributions c_1 and c_2 due to τ_1 and τ_2 could, however, be estimated from the χ'_{ij}/χ_{oij} and χ''_{ij}/χ_{oij} of Fröhlich's eqs. (4.8) and (4.9) and placed in Table 4.3 assuming a continuous distribution of τ between limiting values of τ_1 and τ_2. c_1 and c_2 are also calculated in terms of fixed values of $(\chi'_{ij}/\chi_{oij})\ w_j \to 0$ and $(\chi''_{ij}/\chi_{oij})\ w_j \to 0$ of the graphical plots of (χ'_{ij}/χ_{oij})– w_j and (χ''_{ij}/χ_{oij})– w_j curves of Figs. 4.5 and 4.6 respectively. All the curves are extrapolated to get the fixed values of (χ'_{ij}/χ_{oij}) and (χ''_{ij}/χ_{oij}) at $w_j \to 0$. They are substituted in the Bergmann's eqs. (4.6) and (4.7) to get c_1 and c_2 for the fixed values of τ_1 and τ_2 respectively. All the c's are placed in Table 4.3 for comparison with Fröhlich's method. Both c_1 and c_2 from Fröhlich's [15] equations are all +ve for all the liquids. But c_2 for DMSO at 25 and 35^{0}C are – ve from the graphical method. The –ve value of c_2 is physically meaningless as they are considered to be the relative contributions towards dielectric relaxation processes. This may indicate that the rotation of whole molecule under hf electric field is not in accord with the flexible part probably due to inertia as observed elsewhere [10,11]. The variation of χ'_{ij}/χ_{oij} and χ''_{ij}/χ_{oij} with w_j as shown in Figs. 4.5 and 4.6 are expected to be concave and convex [10,11] respectively. All the curves of Figs. 4.5 and 4.6 are, however, concave except systems VI (–⊕–) of Fig. 4.6. This type of anomalous behaviour in the variation of χ'_{ij}/χ_{oij} and χ''_{ij}/χ_{oij} with w_j invariably demands careful measurement of data in low concentration region.

The dipole moments μ_1 and μ_2 are also calculated from the slope β_1 of χ'_{ij}– w_j curve of Fig. 4.4 and estimated τ_1 and τ_2 as shown in Table 4.4. They are compared with μ_j's from τ_j's of eqs. (4.4) and (4.5) respectively. μ_j's from Gopala Krishna's method [16] and conductivity measurement technique [9] are also reported and placed in Table 4.4 for comparison among them. The total hf conductivity σ_{ij} is plotted against w_j 's of the polar–nonpolar liquid mixture as seen in Fig. 4.7 only to show that all the curves are parabolic in nature exhibiting maximum conductivity at lower temperature and higher concentration for DMSO. At $w_j \to 0$, the curves are found to yield different value of σ_{ij} probably due to the term $1/(M_jT)$ in the eq. (4.28) as seen in Fig. 4.7. The difference in estimated μ_2 and μ_1 from conductivity and susceptibility measurements suggests the involvement of bound molecular charges towards

μ's of polar liquid. It is evident from Table 4.4 that μ_1's of the polar liquids are found to be in excellent agreement with the reported μ's. It thus reveals that a part of the molecule is rotating under 10 GHz electric field as observed earlier [24]. The variation of μ_1 and μ_2 with temperature for DMSO is given by eq. (4.10). The convex nature of μ_1–t equation reveals the fact that the molecule DMSO attains higher asymmetry of larger μ_1 at a certain temperature. It also shows zero dipole moments at two different temperatures indicating the symmetric nature of the molecule. The variation of μ_1 with temperature may occur due to elongation of bond moments. This further invites the extensive study of the relaxation phenomena of highly nonspherical dipolar molecules at different experimental temperatures and in different solvents.

The theoretical dipole moment μ_{theo}'s of the polar molecules are calculated assuming the planar structure from the available bond moments of 7.83 X 10^{-30} C.m., 5.17 X 10^{-30} C.m. for polar groups S←CH_3, O⇐S in DMSO 2.13 X 10^{-30} C.m., 2.60 X 10^{-30} C.m., 1.23 X 10^{-30} C.m. of N←CH_3, N←C_2H_5, CH_3←C in DMF, DEF and DMA respectively. The other bond moments are 1 X 10^{-30} C.m., 1.50 X10^{-30} C.m., 10.33 X 10^{-30} C.m. for C←H, C←N and C⇐O in them. The bond moments are, however, reduced by a factor μ_1/μ_{theo} to yield exact μ's as sketched in Fig. 4.8. The reduction or elongation in bond moments of the substituent polar groups may occur due to inductive, mesomeric and electromeric effects which in turn subsequently act as pusher or puller of electrons in them. The solvent C_6H_6 is a cyclic and planar compound and has three double bonds and six p-electrons on six C-atoms. The dipolar liquid molecules are aliphatic and planar ones. Hence π-π interaction or resonance effect combined with inductive effect commonly known as mesomeric effect in excited state called the electromeric effect may play the vital role in the estimation of μ_{theo} 's of Fig. 4.8.

The thermodynamic energy parameters like enthalpy of activation ΔH_τ entropy of activation ΔS_τ and free energy of activation ΔF_τ of DMSO were calculated from the slope and intercept of $\ln(\tau_1 T)$ against (1/T) of eq. (4.11) on the basis of Eyrings theory considering the rotation of the polar molecule as a rate process. Unlike $\ln(\tau_2 T)$ against (1/T); $\ln(\tau_1 T)$ against (1/T) of DMSO is in accord with the Eyring's rate theory [20]. The value of ΔH_τ for DMSO is 6.85 in KJ $mole^{-1}$ ΔS_τ are –8.21, –8.15, –11.65, –11.48 in J $mole^{-1}$ K^{-1} and ΔF_τ are 9.30, 9.32 , 10.43 and 10.45. at 25, 30, 35 and 40°C respectively in KJ $mole^{-1}$. It is observed that ΔS_τ are –ve indicating the activated states are more ordered than the normal states especially for DMSO.

4.6. CONCLUSION

The study of relaxation phenomena of aprotic polar liquids of amides in C_6H_6 in terms of the modern established symbols of dielectic terminologies and parameters of orientational susceptibilities χ_{ij}'s measured under a single frequency electric field is very encouraging and interesting. It seems to be more topical, significant and useful contribution to predict the conformational structures and various molecular associations of the molecules at any given temperatures. The intercept and slope of derived linear eq.(4.3) on the measured data of χ_{ij} of different w_j's are used to get τ_2 and τ_1. The prescribed methodology in S I units is superior because of the unified, coherent and rationalised nature because χ_{ij}'s are directly linked only with orientational polarization of the molecules. The significant eqs (4.4) and (4.5) to obtain values of τ_j and hence values of μ_j from eq. (4.22) help the future workers to shed more light on the relaxation phenomena of complicated nonspherical polar liquids and liquid crystals. The present method to obtain values of τ_j from eq.(4.5) with the use of the ratio of the individual slopes of χ''_{ij} versus w_j and χ'_{ij} versus w_j curves at $w_j \rightarrow 0$ is a significant improvement over the existing ones, as it eliminates polar-polar interaction almost completely in τ_j's and μ_j's respectively.

The values of τ_j and μ_j are usually claimed to be accurate within 10% and 5% respectively. The tested correlation coefficients r's and % of errors of eq.(4.3) demand that τ and μ are more than accurate. The DMSO, DMF, DMA and DEF molecules absorb electric energy much more strongly under nearly 10 GHz electric field, at which the variation of χ''_{ij} against frequency ω seem to be large. This at once indicates the attention to get the double relaxation phenomena from eq.(4.3). The sum of the experimental and theoretical values of weighted contributions c_1 and c_2 towards dielectric dispersions due to estimated τ_2 and τ_1 differ significantly to indicate more than two Debye type relaxations in such molecules because of their complexity. It can, further, be observed that only a part of the molecule is rotating under nearly 10 GHz electric field since $\ln(\tau_1 T)$ against 1/T obeys the Eyring's rate theory. The values of μ_2 and μ_1 due to τ_2 and τ_1 are expected to be smaller when they are measured from susceptibility measurement technique rather than the hf conductivity and permittivity methods, where approximation of $\sigma_{ij} \approx \sigma'_{ij}$ is usually made. The measurement of μ's from hf conductivities σ_{ij}'s and hf permittivities ε_{ij}'s is involved with the contributions of the bound molecular charges and all types of polarisations including the fast one. The difference

of μ_1 and μ_j from μ_{theo} may arise, either by elongation or reduction of the bond moments of the substituted polar groups by factor μ_1/μ_{theo} in agreement with the measured μ's to take into account of the inductive, mesomeric and electromeric effects of the substituted polar groups in the molecules under investigation. Thus the correlation between the conformational structures with the observed results enhances the scientific content to add a new horizon of understanding the existing knowledge of dielectric relaxation phenomena.

Table 4.1: The real χ'_{ij} and imaginary χ''_{ij}, parts of the complex dielectric orientational susceptibility χ_{ij}^* and static dielectric susceptibility χ_{oij} which is real for various weight fractions w_j's of some aprotic polar liquids in benzenes at different temperatures under hf electric field.

System with sl. no	Temp. in °C	Weight fraction w_j	χ'_{ij}	χ''_{ij}	χ_{oij}
I. DMSO	25	0.0022	0.0611	0.0280	0.0731
		0.0043	0.0890	0.0420	0.1094
		0.0047	0.0950	0.0460	0.1181
		0.0069	0.1231	0.0616	0.1594
		0.0086	0.1520	0.0798	0.1982
II. DMSO	30	0.0022	0.0630	0.0274	0.074
		0.0043	0.0915	0.0400	0.1095
		0.0047	0.0980	0.0440	0.1220
		0.0069	0.1155	0.0526	0.1500
		0.0086	0.1340	0.0648	0.1802
III. DMSO	35	0.0022	0.0600	0.0234	0.0693
		0.0043	0.0800	0.0330	0.108
		0.0047	0.0825	0.0360	0.1135
		0.0069	0.1104	0.0496	0.1564
		0.0086	0.1260	0.0580	0.1830
IV. DMSO	40	0.0022	0.0499	0.0170	0.0648
		0.0043	0.0774	0.0282	0.1054
		0.0047	0.0784	0.0286	0.1094
		0.0069	0.1083	0.0420	0.1541
		0.0086	0.1155	0.0500	0.1775
V. DEF	30	0.0023	0.0850	0.0256	0.1137
		0.0042	0.0899	0.0288	0.1335
		0.0079	0.0997	0.0384	0.1822
		0.0095	0.1033	0.0448	0.2053
VI. DMF	25	0.0027	0.0742	0.0256	0.0948
		0.0036	0.0872	0.0302	0.1162
		0.0048	0.1045	0.0386	0.1423
		0.0063	0.1291	0.0484	0.1855
VII. DMA	25	0.0026	0.0818	0.0213	0.1201
		0.0045	0.1046	0.0278	0.1559
		0.0056	0.1198	0.0330	0.1851
		0.0066	0.1370	0.0381	0.2083

Table 4.2: The relaxation times τ_2 and τ_1 from the slope and intercept of straight line eq. (4.3), measured τ_j from different methods of susceptibility and conductivity measurement technique, reported τ, symmetric and characteristic relaxation times τ_s and τ_{cs} for different aprotic polar liquids under effective dispersive region of nearly 10 GHz electric field.

System	Temp in °C	Estimated τ_1 and τ_2 in ps		τ_j^a in ps	τ_j^b in ps	τ_j^c in ps	τ_j^d in ps	Rept* τ_j in ps	τ_s in ps	τ_{cs} in ps
		τ_1	τ_2							
I. DMSO	25	8.09	21.07	9.91	6.79	8.77	6.01	5.37	4.88	3.69
II. DMSO	30	7.51	52.02	9.07	6.34	8.04	5.86	4.96	4.82	3.05
III. DMSO	35	6.50	59.68	9.08	9.03	7.47	8.95	4.70	4.21	--
IV. DMSO	40	4.51	39.00	8.38	4.90	7.09	4.46	4.33	3.74	22.20
V. DEF	30	3.89	76.41	16.86	1.06	6.64	0.58	2.42	4.16	15.66
VI. DMF	25	4.60	56.24	6.73	6.69	5.87	5.58	5.09	3.02	8.47
VII. DMA	25	2.20	56.61	3.05	6.53	4.96	3.11	6.53	3.90	81.95

τ_j^a = relaxation time from direct slope of eq (4.4)
τ_j^b = relaxation time from ratio of individual slope of eq (4.5)
τ_j^c = relaxation time from direct slope of eq (4.25)
τ_j^d = relaxation time from ratio of individual slope of eq (4.26)
* reported τ_j by using Gopalakrishna's [16] method.

Table 4.3: Fröhlich's parameter A [=ln (τ_2/τ_1)], theoretical and experimental values of χ'_{ij}/χ_{oij} & χ''_{ij}/χ_{oij} of Fröhlich eqs (4.8) and (4.9) and from fitting eqs of Figs 4.5 and 4.6 at $w_j \to 0$ respectively, theoretical and experimental relative contributions c_1 and c_2 towards dielectric dispersion due to τ_1 and τ_2, symmetric and asymmetric distribution parameters γ and δ for polar-nonpolar liquid mixtures of some aprotic polar liquids under effective dispersion region of nearly 10 GHz electric field.

System	Temp in °C	A	Theoretical values of χ'_{ij}/χ_{oij} & χ_{ij}''/χ_{oij} from eqs (4.8) & (4.9)		Theoretical values of c_1 and c_2		Experimental values of χ'_{ij}/χ_{oij} & χ''_{ij}/χ_{oij} at $w_j \to 0$ of Figs. 4.5 & 4.6		Experimental values of c_1 and c_2		Estimated values of γ and δ	
					c_1	c_2			c_1	c_2	γ	δ
I. DMSO	25	0.957	0.629	0.466	0.485	0.571	0.874	0.380	1.095	-0.061	-0.07	2.00
II. DMSO	30	1.935	0.449	0.434	0.423	0.933	0.894	0.389	1.049	0.022	-0.08	2.37
III. DMSO	35	2.217	0.454	0.419	0.425	1.043	1.039	0.371	1.192	-0.076	-0.29	--
IV. DMSO	40	2.241	0.611	0.409	0.507	0.794	0.797	0.266	0.803	0.228	0.21	0.36
V. DEF	30	2.978	0.476	0.378	0.443	1.380	0.849	0.247	0.890	0.210	0.17	0.36
VI. DMF	25	2.505	0.497	0.405	0.451	1.086	0.855	0.262	0.921	0.065	0.13	0.61
VII. DMA	25	3.248	0.601	0.357	0.531	1.093	0.724	0.185	0.713	0.338	0.47	0.18

Table 4.4: Slope β_1 of χ'_{ij} vs w_j and β_2 of σ_{ij} vs w_j curves, measured dipole moments μ_2 and μ_1 from susceptibility measurement technique, μ_j 's from Eqs.(22) and (29) respectively, reported dipole moment, theoretical dipole moment μ_{theo} from available bond angles and bond moments expressed in Coulomb.metre (C.m) and the values of μ_1 /μ_{theo} for some aprotic polar liquids in benzene under effective dispersion region of nearly 10 GHz electric field.

System with sl.no. & mol.wt.	Slope of χ'_{ij}-w_j & σ_{ij} - w_j curves		Dipole moments μ_j (x 10^{-30}) in Coulomb.metre								$\frac{\mu_1}{\mu_{theo}}$
			From Eq (22)		μ_j^a	μ_j^b	μ_j^c	μ_j^d	μ_j^r	μ_{theo}	
	β_1	β_2	μ_2	μ_1							
I.DMSO at 25 ^{0}C M_j= 0.078 Kg	10.943	6.280	14.69	10.30	10.75	10.03	11.10	10.48	12.65	15.18	0.67
II.DMSO at 30 ^{0}C M_j= 0.078 Kg	16.440	9.096	36.69	12.64	13.09	12.35	13.31	12.75	12.79	15.18	0.83
III.DMSO at 35^{0}C M_j= 0.078 Kg	8.950	4.621	31.09	9.27	9.79	9.78	9.50	9.82	13.49	15.18	0.61
IV.DMSO at 40 ^{0}C M_j= 0.078 Kg	17.646	9.894	30.37	12.69	13.70	12.82	13.94	13.32	13.73	15.18	0.83
V.DEF at 30^{0}C M_j= 0.101 Kg	2.870	2.922	26.62	5.67	7.91	5.53	8.18	7.58	12.96	13.30	0.42
VI.DMF at 25 ^{0}C M_j= 0.073 Kg	10.938	7.282	33.21	9.37	9.81	9.80	10.54	10.48	12.09	12.73	0.74
VII.DMA at 25 ^{0}C M_j= 0.087 Kg	5.147	2.792	24.97	6.83	7.07	6.89	7.00	6.81	11.26	13.37	0.51

μ_j^a = dipole moment by using τ from the direct slope of Eq (4)
μ_j^b = dipole moment by using τ from the ratio of individual slopes of Eq (5)
μ_j^c = dipole moment by using τ from the direct slope of Eq (25)
μ_j^d = dipole moment by using τ from the ratio of individual slopes of Eq (26)
μ_j^r = reported dipole moment using Gopalakrishna's[16] τ
μ_{theo} = theoretical dipole moment from the available bond moments.

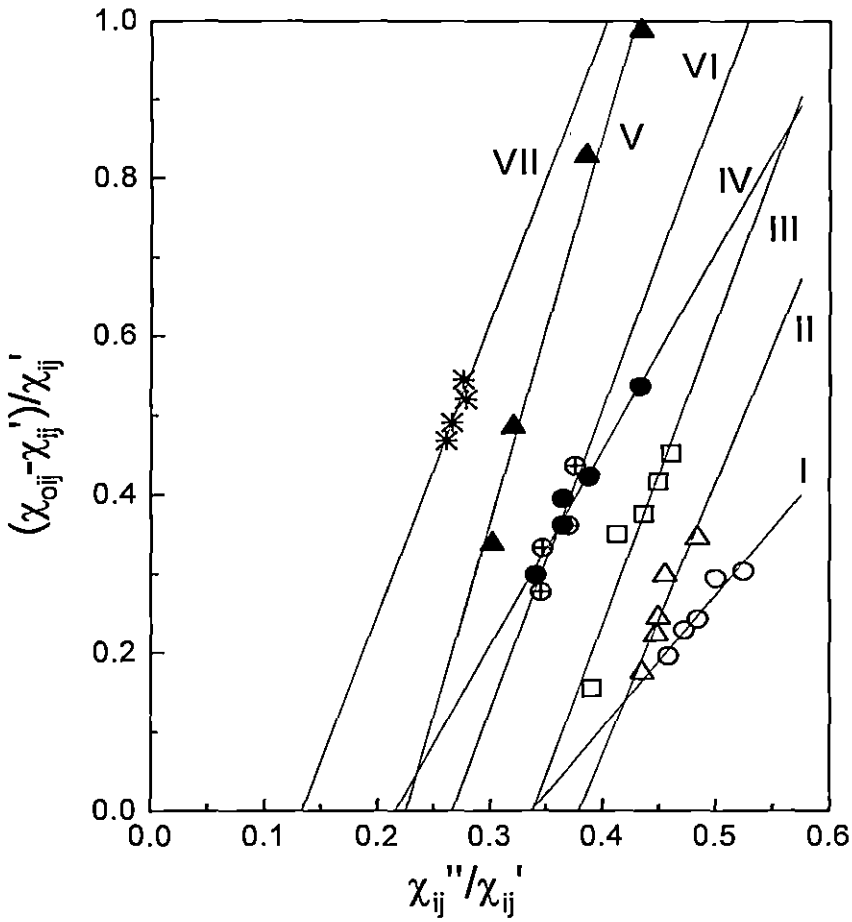

Fig. 4.1: Linear Plot of $(\chi_{oij}-\chi'_{ij})/\chi'_{ij}$ against χ''_{ij}/χ'_{ij} for different w_j's of DMSO, DEF, DMF and DMA in benzene.
(I) DMSO at 25 ^{0}C (-o-),(II) DMSO at 30 ^{0}C (-Δ-),(III) DMSO at 35 ^{0}C (-□-),(IV) DMSO at 40 ^{0}C (-●-),(V) DEF at 30 ^{0}C (-▲-),(VI) DMF at 25 ^{0}C (-⊕-) and (VII) DMA at 25 ^{0}C (-*-).

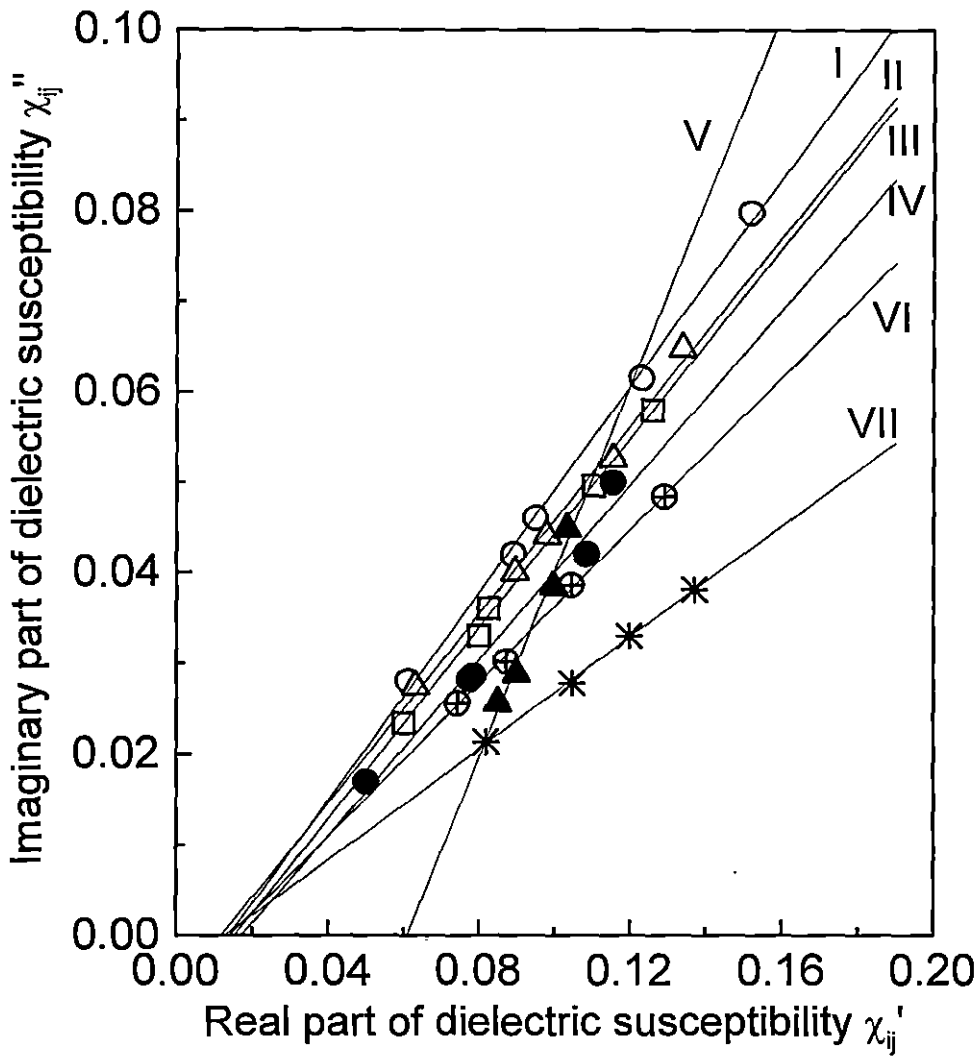

Fig. 4. 2: Linear variation of imaginary part of dielectric susceptibility χ''_{ij} against real part of dielectric susceptibility χ'_{ij} for different w_j's of DMSO, DEF, DMF and DMA in benzene.
(I) DMSO at 25 ^{0}C (-o-),(II) DMSO at 30 ^{0}C (-Δ-),(III) DMSO at 35 ^{0}C (-□-),(IV) DMSO at 40 ^{0}C (-●-),(V) DEF at 30 ^{0}C (-▲-),(VI) DMF at 25 ^{0}C (-⊕-) and (VII) DMA at 25 ^{0}C (-*-).

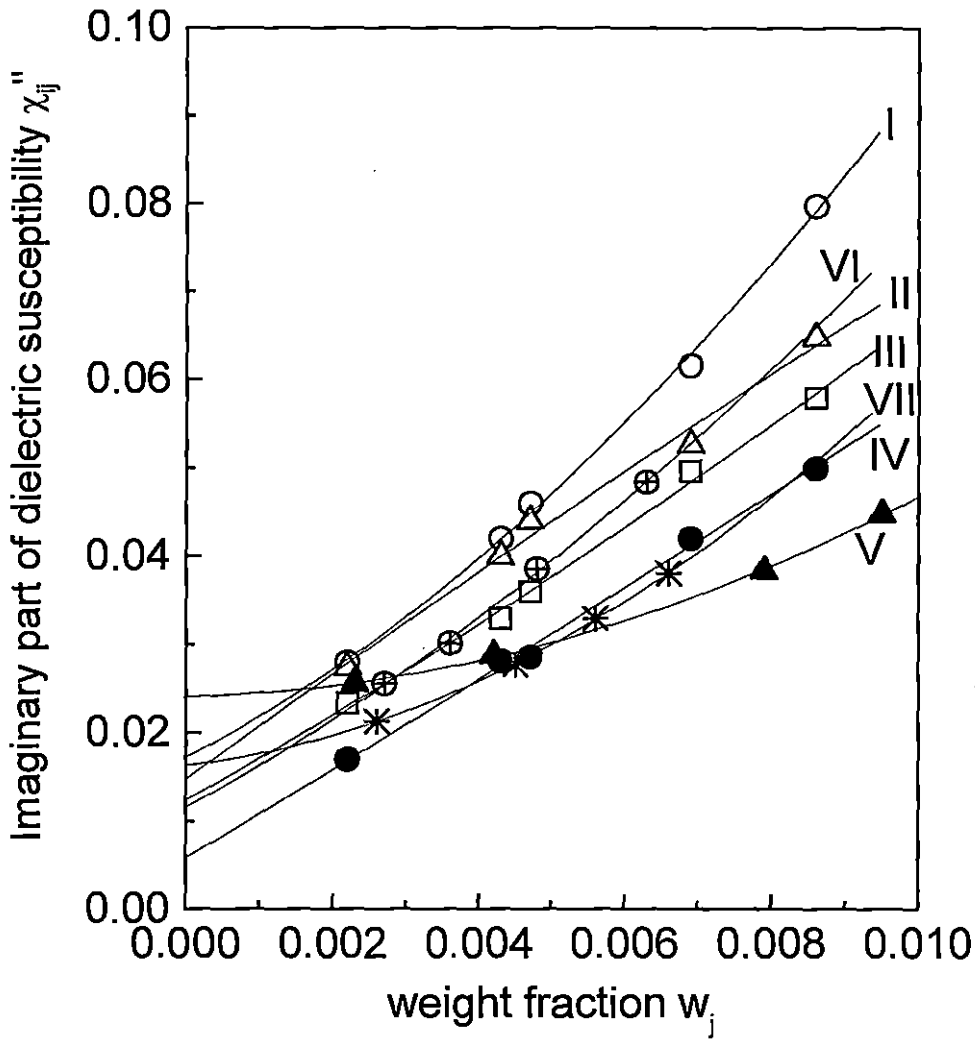

Fig. 4. 3: Plot of imaginary part of dielectric susceptibility χ''_{ij} with weight fraction w_j of DMSO, DEF, DMF and DMA in benzene.
(I) DMSO at 25 ^{0}C (-o-),(II) DMSO at 30 ^{0}C (-Δ-),(III) DMSO at 35 ^{0}C (-□-),(IV) DMSO at 40 ^{0}C (-•-),(V) DEF at 30 ^{0}C (-▲-),(VI) DMF at 25 ^{0}C (-⊕-) and (VII) DMA at 25 ^{0}C (-*-).

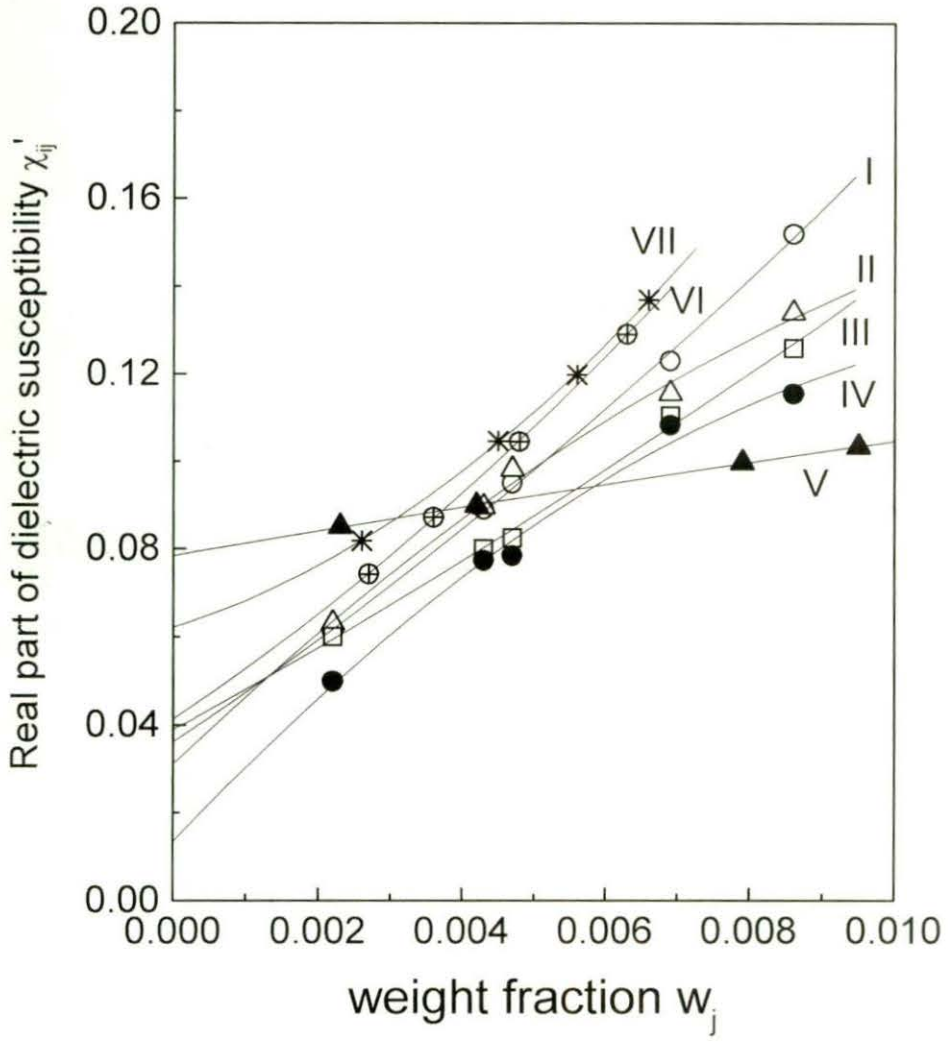

Figure 4.4 Plot of real part of dielectric susceptibility χ_{ij}' with weight fraction w_j of DMSO, DEF, DMF and DMA in benzene.
(I) DMSO at 25 ^{0}C (-o-),(II) DMSO at 30 ^{0}C (-Δ-),(III) DMSO at 35 ^{0}C (-□-),(IV) DMSO at 40 ^{0}C (-●-),(V) DEF at 30 ^{0}C (-▲-),(VI) DMF at 25 ^{0}C (-⊕-) and (VII) DMA at 25 ^{0}C (-*-).

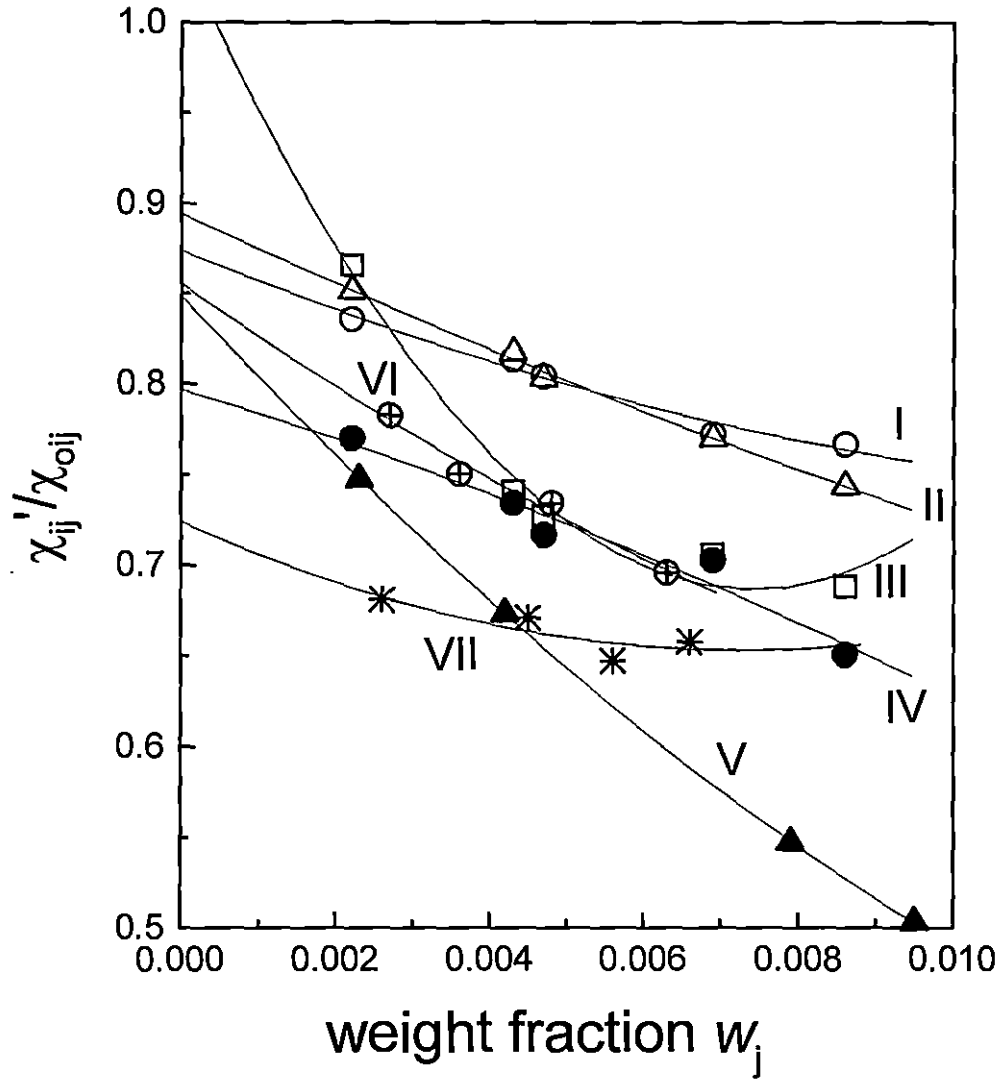

Fig. 4.5: Variation of χ'_{ij}/χ_{oij} with w_j's of DMSO, DEF, DMF and DMA in benzene.
(I) DMSO at 25 ^{0}C (-o-),(II) DMSO at 30 ^{0}C (-Δ-),(III) DMSO at 35 ^{0}C (-□-),(IV) DMSO at 40 ^{0}C (-●-),(V) DEF at 30 ^{0}C (-▲-),(VI) DMF at 25 ^{0}C (-⊕-) and (VII) DMA at 25 ^{0}C (-*-).

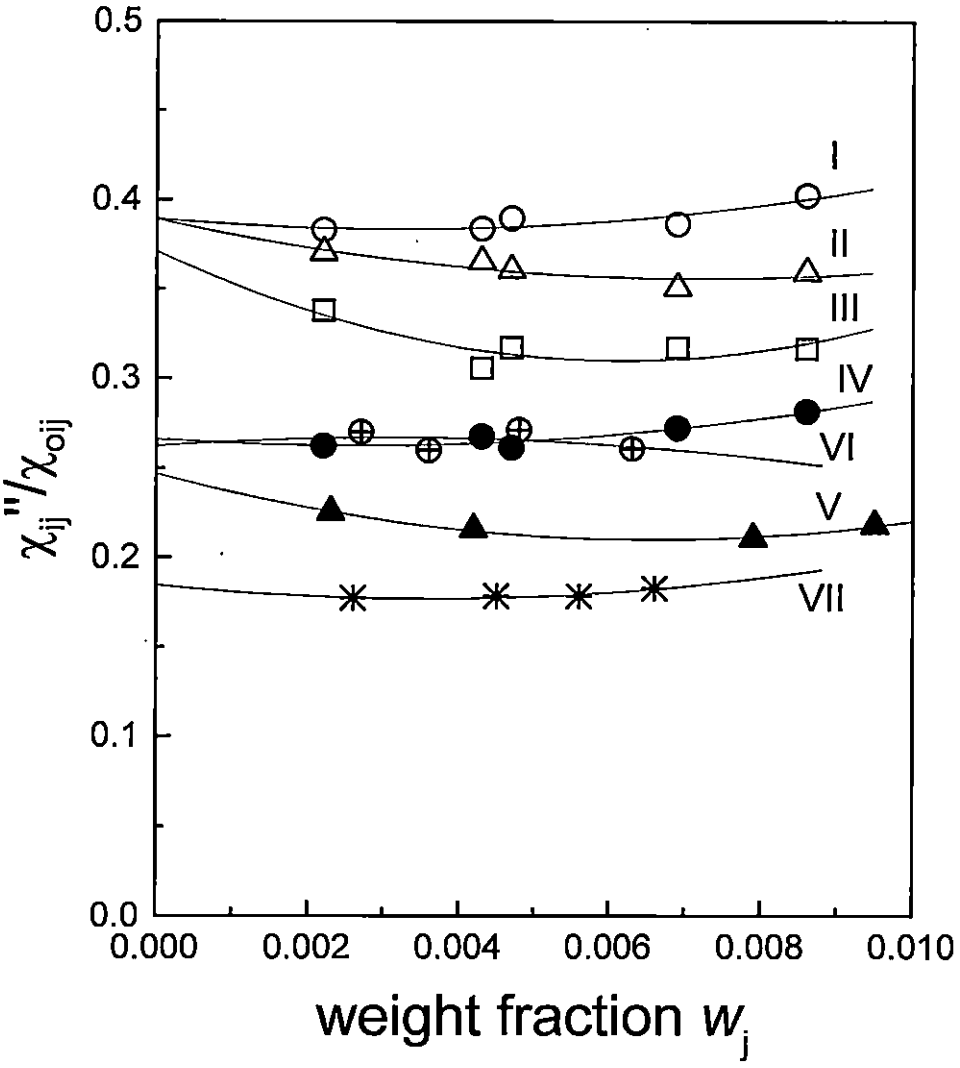

Fig. 4. 6: Variation of χ''_{ij}/χ_{oij} with w_j's of DMSO, DEF, DMF and DMA in benzene.
(I) DMSO at 25 ^{0}C (-o-),(II) DMSO at 30 ^{0}C (-Δ-),(III) DMSO at 35 ^{0}C (-□-),(IV) DMSO at 40 ^{0}C (-●-),(V) DEF at 30 ^{0}C (-▲-),(VI) DMF at 25 ^{0}C (-⊕-) and (VII) DMA at 25 ^{0}C (-*-).

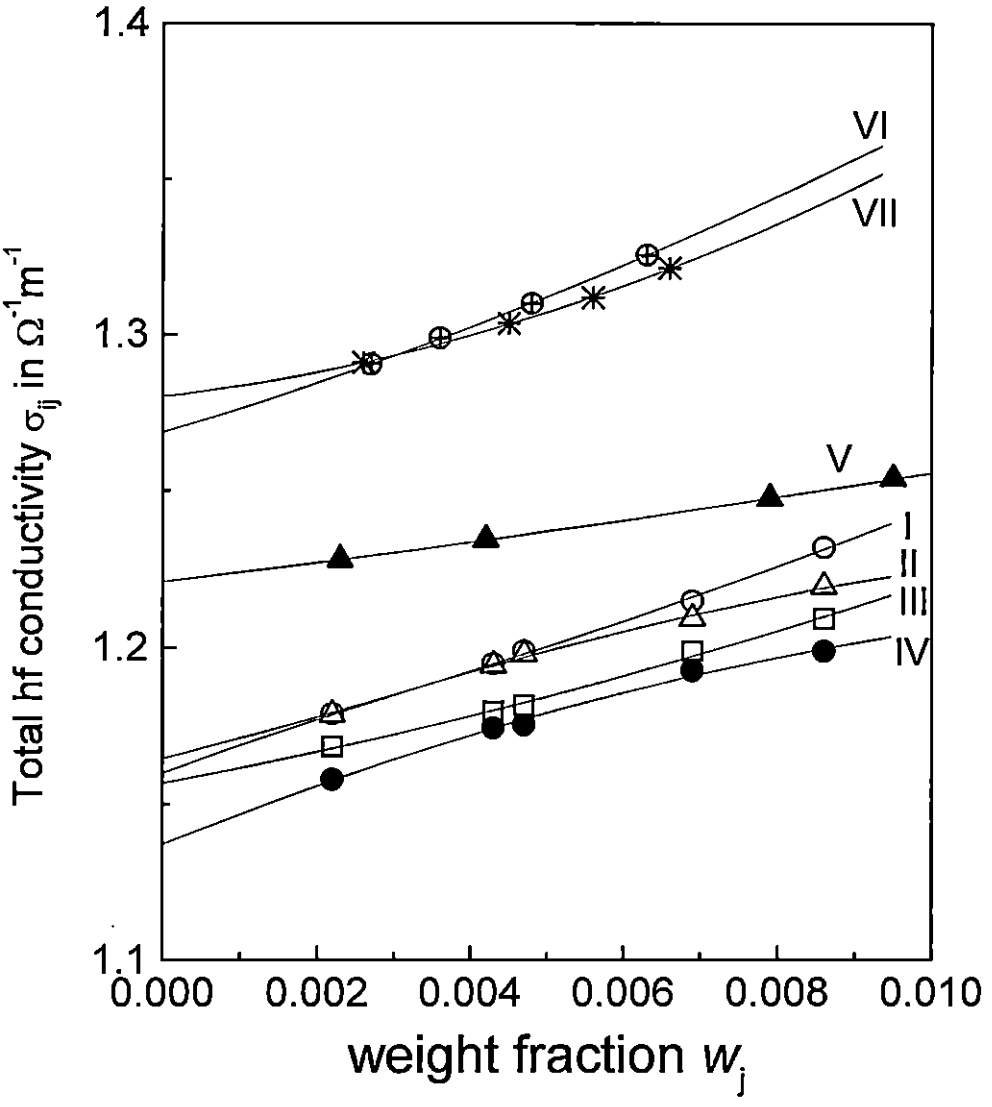

Fig. 4. 7: Variation of total hf conductivity σ_{ij} with w_j's of DMSO, DEF, DMF and DMA in benzene.
(I) DMSO at 25 ^{0}C (-o-),(II) DMSO at 30 ^{0}C (-Δ-),(III) DMSO at 35 ^{0}C (-□-),(IV) DMSO at 40 ^{0}C (-●-),(V) DEF at 30 ^{0}C (-▲-),(VI) DMF at 25 ^{0}C (-⊕-) and (VII) DMA at 25 ^{0}C (-*-).

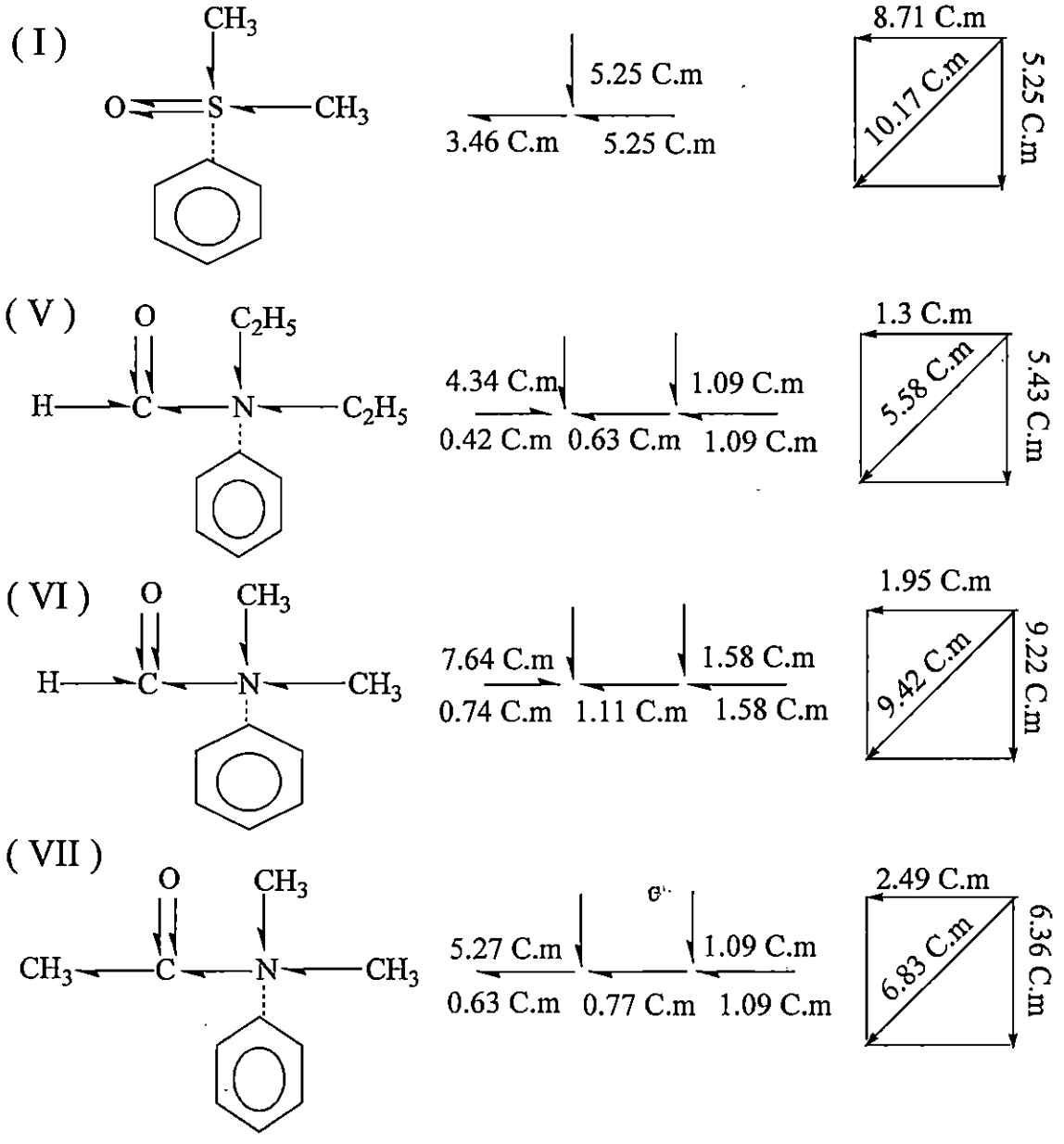

Fig. 4. 8: Conformational structures of aprotic polar liquids in terms of reduced bond length due to mesomeric and inductive moments in Coulomb metre (C.m.)x$10^{30}$of the substituent polar groups:
(I) DMSO (II) DEF (III) DMF (IV) DMA

REFERENCES

[1] S M Puranik, R Y Ghanabahadur, S N Helambe & S C Mehrotra, *Indian J Pure & Appl Phys* **29** (1991) 251

[2] M B R Murthy, B S Dayasagar and R L Patil *Pramana J. Phys* **61** (2003) 725

[3] K K Gupta, A K Bansal, P J Singh & K S Sharma, *Indian J Pure & Appl Phys* **42** (2004) 849

[4] L J Onsager. *Am. Chem.Soc.* **58** (1936) 1485

[5] K Dutta, S K Sit and S Acharyya, *Pramana J. Phys* **57** (2001) 775

[6] N Ghosh, A Karmakar, S K Sit & S Acharyya, *Indian J Pure & Appl Phys* **38** (2000) 574

[7] J S Dhull, D R Sharma and K N Laxminarayana, *Indian J.Phys* **B56** (1982) 334

[8] A Sharma and D R Sharma, *J. Phys. Soc (Japan)* **61** (1992) 1049

[9] S K Sit, K Dutta , S Acharyya, T Pal Majumder and S Roy, *J.Mole Liquids* **89** (2000) 111

[10] S K Sit, N Ghosh, U Saha and S Acharyya, *Indian J. Phys* **71B** (1997) 533

11] U Saha, S K Sit, R C Basak and S Acharyya, *J. PhysD: Appl Phys* (London) **27** (1994) 596

[12] S K Sit, R C Basak, U Saha and S Acharyya, *J. PhysD: Appl Phys* (London) **27**(1994) 2194

[13] A K Jonscher, *Inst. Phys. Conference* Serial No. 58, Invited paper presented at physics of dielectrics Solids 8 – 11 (1980)

[14] T Pal Majumder, *Ph.D thesis* (1996) Jadavpur University, Kolkata

[15] K Bergmann, D M Roberti and C.P Smyth, *J. Phys. Chem* **64** (1960) 665

[16] K V Gopalakrishna, *Trans Faraday Soc.* **53** (1957) 767

[17] H Fröhlich, "*Theory of Dielectrics*" (Oxford university press) 1949

[18] M B R Murthy, R L Patil and D K Deshpande, *Indian J. Phys* **B 63** (1989) 491

[19] K Dutta, A Karmakar, L Dutta, S K Sit & S Acharyya, *Indian J Pure & Appl Phys* **40** (2002) 801

[20] N E Hill, W E Vaughan, A H Price and M Davis " *Dielectric properties and Molecular Behaviour*" Van Nostrand Reinhold company Ltd (London), 1969

[21] C P Smyth, "*Dielectric Behaviour and Structure*" (New York; Mc Graw Hill) 1955

[22] K Dutta, A Karmakar, S K Sit & S Acharyya, *Indian J Pure & Appl Phys* **40** (2002) 588

[23] S K Sit and S Acharyya, *Indian j. pure & appl. Phys* **34** (1996) 255

[24] R C Basak, S K Sit and S Acharyya, *Indian J. Phys.* **B70** (1996) 37